Eur. Phys. J. C (2018) 78:227
https://doi.org/10.1140/epjc/s10052-018-5694-3

THE EUROPEAN PHYSICAL JOURNAL C

CrossMark

Regular Article - Theoretical Physics

Status of quarkonia-like negative and positive parity states in a relativistic confinement scheme

Tanvi Bhavsar[1,a], **Manan Shah**[2,b], **P. C. Vinodkumar**[1,c]

[1] Department of Physics, Sardar Patel University, Vallabh Vidyanagar 388120, India
[2] P D Patel Institute of Applied Sciences, CHARUSAT, Changa 388421, India

Received: 25 October 2017 / Accepted: 3 March 2018 / Published online: 16 March 2018
© The Author(s) 2018

Abstract Properties of quarkonia-like states in the charm and bottom sector have been studied in the frame work of relativistic Dirac formalism with a linear confinement potential. We have computed the mass spectroscopy and decay properties (vector decay constant and leptonic decay width) of several quarkonia-like states. The present study is also intended to identify some of the unexplained states as mixed P-wave and mixed S–D-wave states of charmonia and bottomonia. The results indicate that the X(4140) state can be an admixture of two P states of charmonium. And the charmonium-like states X(4630) and X(4660) are the admixed state of S–D-waves. Similarly, the $X(10610)$ state recently reported by Belle II can be mixed P-states of bottomonium. In the relativistic framework we have computed the vector decay constant and the leptonic decay width for S wave charmonium and bottomonium. The leptonic decay widths for the $J^{PC} = 1^{--}$ mixed states are also predicted. Further, both the masses and the leptonic decay width are considered for the identification of the quarkonia-like states.

1 Introduction

In recent years remarkable experimental progress has been achieved in the investigation of charmonium-like and bottomonium-like states. The latest experimental results on heavy flavor hadrons have gained renewed interest in heavy flavor physics [1,2] to understand the properties of strongly interacting hadrons. Conditions seemed to be very different for spectra above and below the flavor threshold region. In the region above the open-charm threshold, a number of charmonium-like states (the so-called "X Y Z" states) have been discovered with unusual properties. These states might be exotic states, mesonic molecules or multi-quark states [1].

Most of these unknown states do not fit in the standard charmonium and bottomonium spectra [3,4]. All the narrow charmonium states below the open-charm threshold have been observed experimentally and their mass spectrum can be well described by potential models [5]. We have sufficient knowledge of $\eta_c(1S)$ and $\eta_c(2S)$. The BESIII/BEPCII facility in Beijing has shed more light on these spin-singlet states by collecting a new record of $\psi(3686)$ decays in electron–positron annihilations [6]. Recently, BESIII showed that the Y(4260) is split up into two resonant states: one with a mass of $4222.0 \pm 3.1 \pm 1.4$ MeV/c^2 and the other with a mass of $4320.0 \pm 10.4 \pm 7.0$ MeV/c^2 in their cross section measurement of $e^+e \to +J/\psi$ for center of mass energies from $\sqrt{s} = 3.77$–4.60 GeV [7]. A large amount of data on charmonium and bottomonium production is available at RHIC [8–12] and at the LHC [13–19], significantly extending our understanding of quarkonium production in deconfined matter [20]. To understand all these, we have to go beyond the conventional quark or quark–anti-quark bound systems. There are various issues related to higher excited states which are still to be resolved. In this context, phenomenological models either non-relativistic quark model (NRQM) or the relativistic quark model have been developed to study the properties of heavy mesons (charmonium and bottomonium) [21–23].

In the present study we compute the masses of charmonium-like and bottomonium-like states in a relativistic frame work. The mass spectroscopy of charmonium and bottomonium states is observed experimentally with high accuracy [2]. But the masses of the S-wave charmonium states beyond 3S and the bottomonium states beyond 4S are not very well resolved. There are many other X, Y and Z states above the $c\bar{c}$ and $b\bar{b}$ threshold which also are required to be identified. For example $\psi(3770)$, $Y(4008)$, $Y(4220)$, $Y(4260)$, $Y(4330)$, $Y(4360)$, $X(4630)$, $Y(4660)$, $X(10610)$, $Y_b(10880)$ have the same J^{PC} value 1^{--} and this justifies

[a] e-mail: tanvibhavsar1992@yahoo.com
[b] e-mail: mnshah09@gmail.com
[c] e-mail: p.c.vinodkumar@gmail.com

Table 1 Experimental status of some of the negative parity and positive parity quarkonia-like states

Exp. state	Exp. mass (MeV)	J^P	Process (mode)	Experiment
Y (4008)	4008^{+121}_{-49}	1^-	$e^+e^- \to \gamma(\pi^+\pi^- J/\psi)$	Belle [26]
$\psi(4160)$	4191 ± 5	1^-	$e^+e^- \to \eta J/\psi$	Belle [27]
Y (4220)	$4222.0 \pm 3.1 \pm 1.4$	1^-	$e^+e^- \to \gamma(\pi^+\pi^- J/\psi)$	BESIII [7]
Y (4260)	4263^{+8}_{-9}	1^-	$e^+e^- \to \gamma(\pi^+\pi^- J/\psi)$	BABAR [28,29], CLEO [30], Belle [26]
			$e^+e^- \to (\pi^+\pi^- J/\psi)$	CLEO [31]
			$e^+e^- \to (\pi^0\pi^0 J/\psi)$	CLEO [31]
Y (4330)	$4320.0 \pm 10.4 \pm 7.0$	1^-	$e^+e^- \to \gamma(\pi^+\pi^- J/\psi)$	BESIII [7]
Y (4360)	4361 ± 13	1^-	$e^+e^- \to \gamma(\pi^+\pi^- \psi(2S))$	BABAR [32], Belle [33]
X(4630)	4634^{+9}_{-11}	1^-	$e^+e^- \to \gamma(\wedge_c^+ \wedge_c^-)$	Belle [34]
Y (4660)	4664 ± 12	1^-	$e^+e^- \to \gamma(\pi^+\pi^- \psi(2S))$	Belle [33]
$Y_b(10888)$	10888.4 ± 3.0	1^-	$e^+e^- \to \gamma(\pi^+\pi^- \Upsilon(nS))$	Belle [35,36]
$X(10610)$	10609 ± 4.0	1^+	$e^+e^- \to \Upsilon(2S)/\Upsilon(3S)\pi^0\pi^0$	Belle [2]
$h_c(1P)$	3525.41 ± 0.16	1^+	$\psi(2S) \to \pi^0(\gamma\eta_c(1S))$	CLEO [40,41]
$h_b(2P)$	$10259.8^{+1.5}_{-1.2}$	1^+	$\Upsilon(5S) \to \pi^+\pi^-(...)$	Belle [42]
$X(3940)$	$3942^{+7}_{-6} \pm 6$	$?^?$	$e^+e^- \to J/\psi X$	Belle [2]
$X(4020)$	$4025.5^{+2.0}_{-4.7} \pm 3.1$	$?^?$	$e^+e^- \to (D^*\bar{D}*)^0\pi^0$	BESIII [2]
$X(4140)$	$4143 \pm +2.9 \pm 1.2$	$?^?$	$B^+ \to J/\psi\phi K^+$	CDF [2]
$X(4350)$	$4350.6^{+4.6}_{-5.1} \pm 0.7$	$?^?$	$e^+e^- \to e^+e^- J/\psi\phi$	BELL [2]

one to see them as belonging to the quarkonia-like states [24]. According to PDG 2016, the earlier states have been now renamed: Y(4260) as X(4260), Y(4360) as X(4360), Y(4660) as X(4660) and $Y_b(10888)$ as $\Upsilon(10860)$. Some of these states can be either hidden charm (X, Y, Z_c) or hidden bottom (Y_b and Z_b) states and are located above the open-charm or open-bottom threshold. It is well known that their decay properties can also throw light on their identity. Thus we incorporate a computation of leptonic decay properties of these 1^{--} states for comprehensive understanding of these quarkonia-like states. The ultimate goal of this study is to describe the status and properties of the X, Y, Z states with the help of a phenomenological model. However, this task is quite challenging, as more and more new quarkonia-like states are observed.

1.1 $J^P = 1^-$ states

In an initial-state radiation (ISR) process, BaBar observed peaks near 4300 MeV/c^2 in the $\pi^+\pi^- J/\psi$ and $\pi^+\pi^-\psi'$ channels. The partial widths for these two decay channels are larger than that required to observe charmonium states. As these states are produced via the ISR process, they have $J^P = 1^-$ [25]. Some of these 1^- states are listed in Table 1.

1.2 $J^P = 1^+$ states

X(3872) was observed by BELLE [2], then after it was confirmed by BABAR [37] and its J^P value 1^+ was determined by LHCb [38]. Another unknown state, Z(4475), which was produced in a charmonium-rich B meson weak decay process, has a mass close to the excited charmonium. It is believed that this state is a strong candidate for the hidden charm tetraquark state [39]. From experimental observations it might be possible that a state with J^P value 1^+ can be a molecular or tetraquark kind of state. In the present study we also look at these states as an admixture of P-waves of quarkonium states. Some of these 1^+ states are also listed in Table 1. The present study, based on relativistic Dirac formalism, is an attempt to understand the quarkonia-like states below and above the $c\bar{c}$ and $b\bar{b}$ states.

The paper is organized as follows. In Sect. 2 we briefly discuss our relativistic quark model based on the Dirac formalism. In Sect. 3, the leptonic decay width and decay constant of 1^{--} quarkonia are computed and the results are compared with the available experimental results and with other theoretical model predictions. Section 4 addresses the mixing of two nearby mesonic states and predicts the status of experimentally known unresolved negative parity and positive parity states. A summary and the conclusion of the present study are presented in Sect. 5.

2 Theoretical frame work

One of the most successful ways to construct the quarkonium system is to solve Dirac equation for the quark and anti-quark

Table 2 Model parameters fitted in our model for the charmonium and bottomonium systems

System parameters	$b\bar{b}$	$c\bar{c}$
Quark mass (in GeV/c^2)	$m_{b/\bar{b}} = 4.67$	$m_{c/\bar{c}} = 1.27$
V_0 (GeV)	$\frac{-0.246}{(n+1)^{1.42}}$	$\frac{-0.146}{(n+1)^{3.01}}$
Potential strength (λ) (GeV^2)	0.18	0.084

in a confinement potential. For the present study we have considered the confinement through a linear potential. The form of the model potential is expressed as

$$V(r) = \frac{1}{2}(1+\gamma_0)(\lambda r^{1.0} + V_0). \tag{1}$$

Here, λ is the strength of the confinement part of the potential [43]. V_0 is a constant negative potential depth [44–46].

The wave function which satisfies the Dirac equation with a general potential is given by [47,48]

$$(\boldsymbol{\alpha}\cdot\mathbf{p} + m_Q)\psi_q(\mathbf{r}) = [E_q - V(r)\gamma_0]\psi_q(\mathbf{r}), \tag{2}$$

$$[\gamma^0 E_q - \boldsymbol{\alpha}.\mathbf{p} - m_q - V(r)]\psi_q(\mathbf{r}) = 0, \tag{3}$$

where

$$\alpha = \begin{pmatrix} 0 & \sigma \\ \sigma & 0 \end{pmatrix}; \quad \gamma^0 = \begin{pmatrix} 1 & 0 \\ 0 & -1 \end{pmatrix}; \quad \gamma^i = \begin{pmatrix} 0 & \sigma_i \\ -\sigma_i & 0 \end{pmatrix}. \tag{4}$$

V(r) is a potential which consists of a scalar + vector part. The main feature to use scalar plus vector potential is that it is applicable for the bound states of both mesons and baryons [43].

The solution of the Dirac equation can be written in two component (positive and negative energies in the zeroth order) form as [44–46,48]

$$\psi_{nlj}(r) = \begin{pmatrix} \psi^{(+)}_{nlj} \\ \psi^{(-)}_{nlj} \end{pmatrix} \tag{5}$$

where

$$\psi^{(+)}_{nlj}(\mathbf{r}) = N_{nlj}\begin{pmatrix} ig(r)/r \\ (\sigma.\hat{r})f(r)/r \end{pmatrix}\mathcal{Y}_{ljm}(\hat{r}) \tag{6}$$

$$\psi^{(-)}_{nlj}(\mathbf{r}) = N_{nlj}\begin{pmatrix} i(\sigma.\hat{r})f(r)/r \\ g(r)/r \end{pmatrix}(-1)^{j+m_j-l}\mathcal{Y}_{ljm}(\hat{r}), \tag{7}$$

and N_{nlj} is the overall normalization constant [44–46,48]. The normalized spin angular part is expressed as

$$\mathcal{Y}_{ljm}(\hat{r}) = \sum_{m_l,m_s}\langle l, m_l, \frac{1}{2}, m_s | j, m_j\rangle Y_l^{m_l}\chi_{\frac{1}{2}}^{m_s}. \tag{8}$$

Here the spinor $\chi_{\frac{1}{2}m_s}$ are eigenfunctions of the spin operators [44–46,48],

$$\chi_{\frac{1}{2}\frac{1}{2}} = \begin{pmatrix} 1 \\ 0 \end{pmatrix}, \quad \chi_{\frac{1}{2}-\frac{1}{2}} = \begin{pmatrix} 0 \\ 1 \end{pmatrix}. \tag{9}$$

The reduced radial parts $g(r)$ and $f(r)$ of the Dirac spinor $\psi_{nlj}(r)$ are the solutions of the equations given by [44–46,48]

$$\frac{\mathrm{d}^2 g(r)}{\mathrm{d}r^2} + \left[(E_D + m_q)[E_D - m_q - V(r)] - \frac{\kappa(\kappa+1)}{r^2}\right]g(r) = 0 \tag{10}$$

and

$$\frac{\mathrm{d}^2 f(r)}{\mathrm{d}r^2} + \left[(E_D + m_q)[E_D - m_q - V(r)] - \frac{\kappa(\kappa-1)}{r^2}\right]f(r) = 0; \tag{11}$$

it is appropriate to define a new quantum number κ [44–46,48] by

$$\kappa = \begin{cases} -(l+1) = -\left(j+\frac{1}{2}\right) & \text{for} \quad j = l+\frac{1}{2}, \\ \\ l = \left(j+\frac{1}{2}\right) & \text{for} \quad j = l-\frac{1}{2}. \end{cases} \tag{12}$$

On converting these equations into dimensionless form [44–47]

$$\frac{\mathrm{d}^2 g(\rho)}{\mathrm{d}\rho^2} + \left[\epsilon - \rho^{1.0} - \frac{\kappa(\kappa+1)}{\rho^2}\right]f(\rho) = 0, \tag{13}$$

$$\frac{\mathrm{d}^2 f(\rho)}{\mathrm{d}\rho^2} + \left[\epsilon - \rho^{1.0} - \frac{\kappa(\kappa-1)}{\rho^2}\right]g(\rho) = 0, \tag{14}$$

where $\rho = \frac{r}{r_0}$ is a dimensionless variable with suitably chosen scale factor $r_0 = \frac{r}{[(E+m)\lambda]^{\frac{-1}{3}}}$ and the corresponding energy eigenvalue is given by [44–46],

$$\epsilon = (E_D - m_q - V_0)(m_q + E_D)^{\frac{1}{3}}\lambda^{\frac{-2}{3}}. \tag{15}$$

The solutions of $f(\rho)$ and $g(\rho)$ are normalized to get [44–46]

$$\int_0^\infty [f^2(\rho) + g^2(\rho)]\mathrm{d}\rho = 1. \tag{16}$$

Now the wave function for the quarkonium system can be constructed by using positive and negative energy solutions of the Dirac equation. The mass of the particular quark–antiquark system can be written as [44–46]

$$M_{Q\bar{Q}} = E_D^Q + E_D^{\bar{Q}} - E_{cm}; \tag{17}$$

here, E_{cm} in general can have a state dependence, which we absorb in our potential parameter V_0. Thus, we make V_0 state dependent.

In these calculations, we incorporate additionally, the j–j coupling, spin–orbit and tensor interactions of confined one gluon exchange potential (COGEP) [43–46]. The mass of the state thus represented by $M_{^{2s+1}L_J}$ as [44–46],

$$M_{^{2s+1}L_J} = M_{Q\bar{Q}}(n_1 l_1 j_1, n_2 l_2 j_2) + \langle V^{j_1 j_2}_{Q\bar{Q}}\rangle + \langle V^{LS}_{Q\bar{Q}}\rangle + \langle V^{T}_{Q\bar{Q}}\rangle \tag{18}$$

Table 3 S-wave mass spectrum for $b\bar{b}$ and $c\bar{c}$ bound states (in MeV)

Bottomonium							
nL	State	Present	Experimental [2]	[50]	[51]	[52]	[53]
1S	1^3S_1	9460.99	9460.30 ± 0.26	9460.43	9460.38	9460	9608
	1^1S_0	9390.7	9399.0 ± 2.3	9392.38	9392.91	9390	9607
2S	2^3S_1	10024.1	10023.26 ± 0.31	10023.80	10023.3	10015	10023.3
	2^1S_0	9999.3	...	9990.88	9987.42	9990	...
3S	3^3S_1	10356.2	10355.2 ± 0.5	10345.80	10364.2	10343	10353.3
	3^1S_0	10325.3	...	10323.40	10333.9	10326	...
4S	4^3S_1	10576.2	10579.4 ± 1.2	10575.20	10636.4	10597	10580
	4^1S_0	10554.4	...	10558.30	10609.4	10584	...
5S	5^3S_1	10758.5	...	10755.40	...	10811	10865
	5^1S_0	10738.4	...	10741.40	...	10800	...
Charmonium							
nL	State	Present	Experimental [2]	[50]	[54]	[55]	[53]
1S	1^3S_1	3096.7	3096.90 ± 0.006	3097.14	3097	3090	3096.9
	1^1S_0	2977.8	2983.4 ± 0.5	2979	2982	2979	
2S	2^3S_1	3684.4	3686.097 ± 0.025	3689.95	3673	3672	3686
	2^1S_0	3630.5	3639.2 ± 1.2	3633.49	3623	3630	...
3S	3^3S_1	4022.4	...	4030.32	4022	4072	3769.9
	3^1S_0	3990.8	...	3991.99	3991	4043	...
4S	4^3S_1	4266.4	...	4273.49	4273	4406	4040
	4^1S_0	4262.1	...	4244.11	4250	4384	...
5S	5^3S_1	4441.5	...	4464.12	4463	4159	...
	5^1S_0	4439.2	...	4440.12	4446	...	...

where the j–j coupling term is expressed as [43,44,44–46,49]

$$\langle V^{j_1 j_2}_{Q\bar{Q}} \rangle = \frac{\sigma \langle j_1 j_2 JM | \widehat{j_1}\widehat{j_2} | j_1 j_2 JM \rangle}{(E_Q + m_Q)(E_{\bar{Q}} + m_{\bar{Q}})}; \tag{19}$$

here, σ is the j–j coupling constant. $\langle j_1 j_2 JM | \widehat{j_1}\widehat{j_2} | j_1 j_2 JM \rangle$ contains the square of the Clebsch–Gordan coefficient. The spin–orbit interaction and tensor interactions are expressed, respectively, by [43–46,49]

$$\begin{aligned}\langle V^{LS}_{Q\bar{Q}} \rangle = \frac{\alpha_s}{4} \frac{N_Q^2 N_{\bar{Q}}^2}{(E_Q + m_Q)(E_{\bar{Q}} + m_{\bar{Q}})} \frac{\lambda_Q \lambda_{\bar{Q}}}{2r} \\ \otimes [[\overrightarrow{r} \times (\widehat{p}_Q - \widehat{p}_{\bar{Q}}).(\sigma_Q - \sigma_{\bar{Q}})](D_0'(r) + 2D_1'(r)) \\ + [[\overrightarrow{r} \times (\widehat{p}_Q + \widehat{p}_{\bar{Q}}).(\sigma_i - \sigma_j)(D_0'(r) - D_1'(r))\end{aligned} \tag{20}$$

and

$$\begin{aligned}\langle V^{T}_{Q\bar{Q}} \rangle = -\frac{\alpha_s}{4} \frac{N_Q^2 N_{\bar{Q}}^2}{(E_Q + m_Q)(E_{\bar{Q}} + m_{\bar{Q}})} \lambda_Q \lambda_{\bar{Q}} \\ \otimes \left(\left(\frac{D_1''(r)}{3} - \frac{D_1'(r)}{3r} \right) S_{Q\bar{Q}} \right)\end{aligned} \tag{21}$$

where $S_{Q\bar{Q}} = [3(\sigma_Q.\hat{r})(\sigma_{\bar{Q}}.\hat{r}) - \sigma_Q.\sigma_{\bar{Q}}]$ and $\hat{r} = \hat{r}_Q - \hat{r}_{\bar{Q}}$ is the unit vector in the relative coordinate [44–46].

Table 4 P-wave mass spectrum for $b\bar{b}$ and $c\bar{c}$ bound states (in MeV)

Bottomonium							
nL	State	Present	Experimental [2]	[50]	[51]	[52]	[53]
1P	1^3P_2	9912.3	9912.21 ± 0.26	9907.89	9912.3	9921	9812
	1^3P_1	9901.8	9892.78 ± 0.26	9887.63	9904.7	9903	9812
	1^3P_0	9889.2	9859.44 ± 0.42	9862.29	9861.39	9864	9811
	1^1P_1	9854.1	9899.3 ± 0.8	9896.07	9899.93	9909	9812
2P	2^3P_2	10265.9	10268.65 ± 0.22	10267.65	10271.2	10264	10044
	2^3P_1	10258.9	10255.46 ± 0.22	10255.74	10254.8	10249	10043
	2^3P_0	10234.7	10232.50 ± 0.40	10240.85	10230.5	10220	10042
	2^1P_1	10264.9	...	10260.70	10261.8	10254	10043
3P	3^3P_2	10516.9	...	10516.28	...	10528	10272
	3^3P_1	10508.8	10512.1 ± 2.3	10507.24	...	10515	10271
	3^3P_0	10497.6	...	10497.07	...	10490	10270
	3^1P_1	10540.2	...	10511.30	...	10519	...
4P	4^3P_2	10707.0	...	...	...	...	...
	4^3P_1	10706.5	...	...	...	...	...
	4^3P_0	10703.8	...	...	...	...	...
	4^1P_1	10704.6	...	...	...	...	...
Charmonium							
nL	State	Present	Experimental [2]	[50]	[54]	[55]	[53]
1P	1^3P_2	3554.2	3556.20 ± 0.09	3570.00	3554	3556	3467
	1^3P_1	3513.0	3510.66 ± 0.07	3490.94	3510	3505	3468
	1^3P_0	3418.4	3414.75 ± 0.31	3392.11	3433	3424	3468
	1^1P_1	3518.7	3525.38 ± 0.11	3523.88	3519	3516	3467
2P	2^3P_2	3921.2	3927.2 ± 2.6	3949.01	3937	3972	3815
	2^3P_1	3901.8	...	3902.55	3901	3925	3815
	2^3P_0	3824.9	...	3844.49	3842	3852	3814
	2^1P_1	3956.2	...	3921.91	3908	3934	3815
3P	3^3P_2	4203.7	...	4211.78	4208	4317	4163
	3^3P_1	4174.6	...	4178.47	4178	4271	4162
	3^3P_0	4136.0	...	4136.84	4131	4202	4160
	3^1P_1	4231.1	...	4192.35	4184	4279	...
4P	4^3P_2	4415.1	...	...	...	...	...
	4^3P_1	4409.1	...	...	...	...	...
	4^3P_0	4383.2	...	...	...	...	...
	4^1P_1	4446.4	...	...	...	...	

The running strong coupling constant α_s is computed as [44–46]

$$\alpha_s = \frac{4\pi}{(11 - \frac{2}{3} n_f) \log\left(\frac{E_Q^2}{\Lambda^2_{QCD}}\right)} \tag{22}$$

with $n_f = 3$ and $\Lambda_{QCD} = 0.250$ GeV for charmonium and $n_f = 4$ and $\Lambda_{QCD} = 0.156$ GeV for bottomonium. In Eq. (20)

Table 5 D-wave mass spectrum for $b\bar{b}$ and $c\bar{c}$ bound states (in MeV)

Bottomonium							
nL	State	Present	Experimental [2]	[50]	[51]	[52]	[53]
1D	1^3D_3	10140.4	...	10176.68	10163.1	10157	9980
	1^3D_2	10138.7	10163.7 ± 1.4	10162.26	10157.3	10153	9980
	1^3D_1	10136.0	...	10147.31	...	10146	9980
	1^1D_2	10068.2	...	10166.00	10158.6	10153	9980
2D	2^3D_3	10398.7	...	10447.09	10455.7	10436	10175
	2^3D_2	10397.1	...	10437.52	10450.3	10432	10174
	2^3D_1	10395.7	...	10427.59	...	10425	10174
	2^1D_2	10336.0	...	10440	10451.4	10432	10174
3D	3^3D_3	10620.9	...	10651.86	...	...	...
	3^3D_2	10619.3	...	10644.62	...	...	...
	3^3D_1	10616.8	...	10637.12	...	...	...
	3^1D_2	10564.3	...	10646.50	...	...	...
4D	4^3D_3	10820.9	...	10816.93	...	...	...
	4^3D_2	10819.3	...	10811.09	...	...	...
	4^3D_1	10816.9	...	10805.03	...	...	...
	4^1D_2	10768.8	...	10812.60	...	...	...
5D	5^3D_3	11005.2	...	10955.6	...	...	
	5^3D_2	11003.7	...	10950.7	...	...	
	5^3D_1	11001.4	...	10945.6	...	...	
	5^1D_2	10956.7	...	10952.0	...	...	

Charmonium							
nL	State	Present	Experimental [2]	[50]	[54]	[55]	[53]
1D	1^3D_3	3769.6	...	3843.95	3799	3806	3805
	1^3D_2	3756.1	...	3787.72	3798	3800	3807
	1^3D_1	3745.3	3773.13 ± 0.35	3729.41	3787	3785	3808
	1^1D_2	3662.2	...	3802.30	3796	3799	3806
2D	2^3D_3	4060.7	...	4132.53	4103	4167	4143
	2^3D_2	4048.4	...	4095.17	4100	4158	4145
	2^3D_1	4038.9	...	4056.43	4089	4142	4145
	2^1D_2	3968.9	...	4104.86	4099	4158	4143
3D	3^3D_3	4317.2	...	4350.66	4331	...	...
	3^3D_2	4307.0	...	4322.44	4327	...	...
	3^3D_1	4300.6	...	4293.18	4317	...	...
	3^1D_2	4236.2	...	4329.76	4326	...	...
4D	4^3D_3	4552.0	...	4526.41	...	...	...
	4^3D_2	4541.6	...	4503.63	...	...	...
	4^3D_1	4533.6	...	4480.01	...	...	...
	4^1D_2	4477.6	...	4509.54	...	...	...
5D	5^3D_3	4768.7	...	4673.96	...	...	...
	5^3D_2	4758.9	...	4654.80	...	...	...
	5^3D_1	4751.6	...	4634.92	...	...	...
	5^1D_2	4699.9	...	4659.77	...	...	...

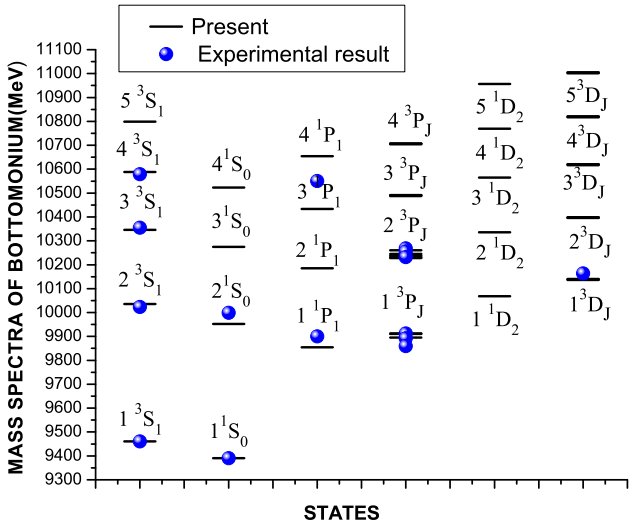

Fig. 1 Mass spectrum of Bottomonium

the spin–orbit term has been split into symmetric $(\sigma_Q + \sigma_{\bar{Q}})$ and anti-symmetric $(\sigma_Q - \sigma_{\bar{Q}})$ terms.

We have adopted the form of the confined gluon propagators which are given by [43–46,49]:

$$D_0(r) = \left(\frac{\alpha_1}{r} + \alpha_2\right) \exp(-r^2 c_0^2/2), \tag{23}$$

$$D_1(r) = \frac{\gamma}{r} \exp(-r^2 c_1^2/2), \tag{24}$$

where $\alpha_1 = 1.035$, $\alpha_2 = 0.3977$, $c_0 = 0.3418$ GeV, $c_1 = 0.4123$ GeV, $\gamma = 0.8639$ are the fitted parameter as in [49]. Other model parameters employed in the present calculation are listed in Table 2.

The hyperfine splittings of ground and radial excitation of the bottomonium and charmonium are important for the study of the radiative transition amplitudes. The high precision experimental data have provided an accurate description of the hyperfine and fine structure interactions of quarkonia. The hyperfine splitting for S-wave and the ratio of the spin–orbit splittings for P-wave charmonium and bottomonium are given by Eqs. (25) and (26), respectively.

$$\triangle M_{hf}(nS) = M(n^3S_1) - M(n^1S_0), \tag{25}$$

$$R = \frac{M(^3P_2) - M(^3P_1)}{M(^3P_1) - M(^3P_0)}. \tag{26}$$

The computed S-wave, P-wave and D-wave mass spectra of bottomonium and charmonium are tabulated in Tables 3, 4 and 5. The corresponding energy level diagrams are shown in Figs. 1 and 2, respectively. The hyperfine splitting for S-wave and the spin–orbit splitting ratio for P-wave is tabulated in Tables 6 and 7.

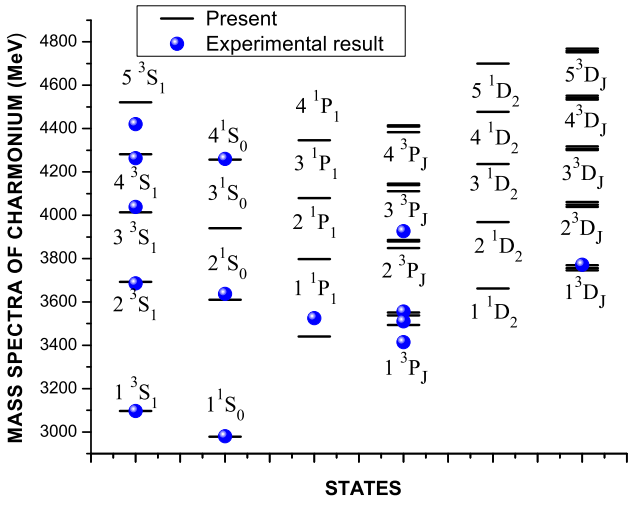

Fig. 2 Mass spectrum of Charmonium

Table 7 The ratios of spin–orbit splittings (R) for P-wave bottomonium and charmonium

Bottomonium				
State (nP)	Present	Experimental [2]	[23]	[50]
1P	0.83	0.60	0.80	0.80
2P	0.29	0.56	0.60	0.80
3P	0.72	...	0.72	0.78
4P	0.18	...	...	...
Charmonium				
State (nP)	Present	Experimental [2]	Lattice QCD [56]	NRp model [56]
1P	0.43	0.47	0.46	0.62
2P	0.25	...	...	0.64
3P	0.75	...	...	...
4P	0. 23	...	...	...

3 Decay constants and leptonic decay width of 1^{--} quarkonia

The leptonic decay width is a tool to understand the compactness of the mesonic system. We know that the leptonic decay width of J/Ψ is reasonably predicted by the phenomenological model. At the same time heavy quarkonium states are precisely most sensitive to the short range one gluon exchange interaction between quarks and anti-quarks [63].

In a relativistic quark model, the vector decay constant is expressed through the meson wave function $f(\overrightarrow{q})$ in momentum space as given by [64]

$$f_V = \frac{2\sqrt{3}}{M}\int \mathrm{d}^3q\left(\frac{m+E}{E} - \frac{\overrightarrow{q}^2}{3E^2})\right) f(\overrightarrow{q}). \tag{27}$$

Here $E = \sqrt{\overrightarrow{q}^2 + m^2}$ and $\sqrt{3}$ is the color factor. M is the mass of vector state. The leptonic decay width is expressed as [64]

$$\Gamma(V \to e^+e^-) = \frac{4}{3}\pi\alpha^2 e_Q^2 \frac{f_V^2}{M}. \tag{28}$$

The computed decay constants and leptonic decay widths in the case of charmonium and bottomonium sates are presented in Tables 8 and 9, respectively. The ratio of $\frac{\Gamma_{ee}(nS)}{\Gamma_{ee}(1S)}$ for bottomonium and charmonium states are listed in Table 10. Along with the mass predictions, the leptonic decay widths are also important for the identification of the structures of quarkonia-like states.

Table 6 The hyperfine splittings (in MeV) for S-wave bottomonium and charmonium

Bottomonium					
State (ns)	Hyperfine splitting	Present	Experimental [2]	[23]	[50]
1S	$\triangle M(1S) = M(1^3S_1) - M(1^1S_0)$	70.2	70	60	68
2S	$\triangle M(2S) = M(2^3S_1) - M(2^1S_0)$	24.8 ($\sim$ 25)	24	30	33
3S	$\triangle M(3S) = M(3^3S_1) - M(3^1S_0)$	30.9 ($\sim$ 31)	...	27	22
4S	$\triangle M(4S) = M(4^3S_1) - M(4^1S_0)$	21.8 ($\sim$ 22)	...	26	17
5S	$\triangle M(5S) = M(5^3S_1) - M(5^1S_0)$	20.1	...	...	14
Charmonium					
State (ns)	Hyperfine splitting	Present	Experimental [2]	Lattice QCD [56]	NRp model [56]
1S	$\triangle M(1S) = M(1^3S_1) - M(1^1S_0)$	118.9 ($\sim$ 119)	116	114	108
2S	$\triangle M(2S) = M(2^3S_1) - M(2^1S_0)$	53.9 ($\sim$ 54)	49	41	42
3S	$\triangle M(3S) = M(3^3S_1) - M(3^1S_0)$	31.6	...	25	29
4S	$\triangle M(4S) = M(4^3S_1) - M(4^1S_0)$	4.3	3	...	...
5S	$\triangle M(5S) = M(5^3S_1) - M(5^1S_0)$	2.3	...	...	...

Table 8 Vector decay constant (F_v in MeV) of the S-wave and D-wave bottomonium and charmonium states

Bottomonium							
State	Present	Experimental [2]	[57]	[58]	[59]	State	Present
1S	705.4	715 ± 5	831	665	867	1D	208.3
2S	554.9	498 ± 8	566	475	673	2D	181.3
3S	436.8	430 ± 4	507	418	595	3D	151.4
4S	332.4	336 ± 18	481	388	549	4D	135.4
5S	286.5	···	458	367	516	5D	113.1
Charmonium							
State	Present	Experimental [2]	[57]	[58]	[60]	State	Present
1S	419.9	416 ± 6	462	393	589	1D	102.5
2S	285	304 ± 4	369	293	328	2D	83.9
3S	218	···	329	258	244	3D	65.6
4S	165.7	···	310	···	···	4D	54.2
5S	106.2	···	290	···	···	5D	42.3

Table 9 Leptonic decay width (in keV) of the S-wave and D-wave bottomonium and charmonium states

Bottomonium							
State	Present	Experimental [2]	[50]	[51]	[43]	State	Our
1S	1.30	1.34 ±0.018	1.203	1.33	1.809	1D	0.106
2S	0.76	0.612 ± 0.011	0.519	0.62	0.797	2D	0.078
3S	0.45	0.443 ± 0.008	0.330	0.48	0.618	3D	0.051
4S	0.26	0.272 ± 0.029	0.241	0.40	0.541	4D	0.042
5S	0.18	···	0.19	···	···	5D	0.028
Charmonium							
State	Present	Experimental [2]	[50]	[61]	[62]	State	Our
1S	5.63	5.55 ± 0.14	4.94	1.89	5.469	1D	0.27
2S	2.19	2.48 ± 0.06	1.686	1.04	2.140	2D	0.17
3S	1.20	···	0.959	0.77	0.796	3D	0.099
4S	0.63	···	0.654	0.65	0.288	4D	0.064
5S	0.24	···	0.489	···	···	5D	0.044

4 Quarkonia-like states as mixed quarkonia states

It is well known that many of the hadronic states which are observed and yet not clear as regards their structure can be the admixture of the nearby iso-parity states. In general, the mass of a mixed state (M_{nL}) can be expressed in terms of the two mixing states (nl and $n'l'$) as

$$M_{nL} = \mid a^2 \mid M_{nl} + (1 - \mid a^2 \mid) M_{n'l'}. \tag{29}$$

Here $\mid a^2 \mid = \cos^2\theta$ and θ is the mixing angle. With the help of this equation we can obtain a mixed state configuration and mixing angle [50]. The computed masses and their leptonic decay widtsh of the S–D-wave admixture states are presented in Table 11. In this context we consider the admixture of nearby P-waves for the predictions of some of the 1^+ states and for other 1^- states we consider the S–D-wave mixing [44,65,66]. The mixed P wave states can be expressed as [44,65,66]

Table 10 The ratios of $\frac{\Gamma_{ee}(nS)}{\Gamma_{ee}(1S)}$ for bottomonium and charmonium states

$\frac{\Gamma_{e^+e^-}(\Upsilon(nS)}{\Gamma_{e^+e^-}(\Upsilon(1S)}$	Present	Experimental [2]	[68]
Bottomonium			
$\frac{\Gamma_{e^+e^-}(2S)}{\Gamma_{e^+e^-}(1S)}$	0.58	0.46	0.50
$\frac{\Gamma_{e^+e^-}(3S)}{\Gamma_{e^+e^-}(1S)}$	0.35	0.33	0.36
$\frac{\Gamma_{e^+e^-}(4S)}{\Gamma_{e^+e^-}(1S)}$	0.20	0.20	0.29
$\frac{\Gamma_{e^+e^-}(5S)}{\Gamma_{e^+e^-}(1S)}$	0.13	···	0.24
Charmonium			
$\frac{\Gamma_{e^+e^-}(2S)}{\Gamma_{e^+e^-}(1S)}$	0.39	0.43	0.48
$\frac{\Gamma_{e^+e^-}(3S)}{\Gamma_{e^+e^-}(1S)}$	0.21	···	0.32
$\frac{\Gamma_{e^+e^-}(4S)}{\Gamma_{e^+e^-}(1S)}$	0.11	···	0.24
$\frac{\Gamma_{e^+e^-}(5S)}{\Gamma_{e^+e^-}(1S)}$	0.04	···	0.19

$$|\alpha\rangle = \sqrt{\frac{2}{3}}|^3P_1\rangle + \sqrt{\frac{1}{3}}|^1P_1\rangle \tag{30}$$

$$|\beta\rangle = -\sqrt{\frac{1}{3}}|^3P_1\rangle + \sqrt{\frac{2}{3}}|^1P_1\rangle. \tag{31}$$

Here $|\alpha\rangle$, $|\beta\rangle$ are states having the same parity. We can write the masses of these states in terms of the predicted masses of the pure P wave states ($^3P_1$ and $^1P_1$) as [44,65,66]

$$M(|\alpha\rangle) = \frac{2}{3}M(^3P_1) + \frac{1}{3}M(^1P_1), \tag{32}$$

$$M(|\beta\rangle) = \frac{2}{3}M(^1P_1) + \frac{1}{3}M(^3P_1). \tag{33}$$

The computed mixed P-wave states for the positive parity quarkonia-like states are listed in Table 12 and the experimental states which are close to these mixed states are also listed for comparison (Table 10).

5 Result and discussion

In the framework of the Dirac relativistic quark model, we have studied the mass spectrum of bottomonium-like and charmonium-like states. To obtain these mass spectra we have solved the Dirac equations with a linear plus constant confinement potential. In our calculations, spin-dependent interactions are included to remove the degeneracy of the states. The predicted bottomonium and charmonium spec-

Table 11 Mixing angle and the leptonic decay widths of S–D-wave admixture states

Experimental state	J^P	mixed state configuration	% mixing of S-wave	Mass of mixed state (MeV) Our	Experimental	Mixed state leptonic decay width (keV) Our	Experimental
Charmonium-like states							
Y(4008)	1^-	2^3S_1 and 2^3D_1	8.6	4008.4	4008^{+121}_{-49} [26]	0.347	0.862 ± 0.241 [72]
$\psi(4160)$	1^-	3^3S_1 and 3^3D_1	39.2	4191	4191 ± 5 [2]	0.534	0.48 ± 0.22 keV [2]
Y(4220)	1^-	3^3S_1 and 3^3D_1	28.7	4220.7	$4222.0 \pm 3.1 \pm 1.4$ [7]	0.417	NA
X(4260)	1^-	3^3S_1 and 3^3D_1	14.41	4260.5	4251 ± 9 [2]	0.258	NA
X(4360)	1^-	4^3S_1 and 4^3D_1	64.97	4360	4346 ± 6 [2]	0.431	< 0.57 eV [2]
X(4630)	1^-	5^3S_1 and 5^3D_1	37.92	4634	4634^{+9}_{-11} [34]	0.117	NA
X(4660)	1^-	5^3S_1 and 5^3D_1	34.37	4645	4643 ± 9 [2]	0.110	<0.45 eV [2]
Bottomonium-like state							
$\Upsilon(10860)$	1^-	5^3S_1 and 5^3D_1	45.45	10880.1	10891 ± 4 [2]	0.096	0.31 ± 0.07 keV [2]

NA not available

Table 12 Masses of mixed P-wave +ve parity states

Experimental state	Mixed state configuration	Present (MeV)
Charmonium-like states		
X(3940)	2^3P_1 and 2^1P_1	3939.06
X(4020)	2^3P_1 and 3^1P_1	4011.56
X(4140)	2^3P_1 and 3^1P_1	4121.33
X(4350)	4^3P_1 and 3^1P_1	4349.76
Bottomonium-like state		
X(10610)	4^3P_1 and 3^1P_1	10595.63

tra are in good agreement with the experimental data and other available theoretical data. We have also predicted the 4S and 5S states for charmonium and bottomonium and compared them with the available theoretical results. The predicted masses of the S-wave bottomonium states 3^3S_1 (10356.2 MeV) and 4^3S_1 (10576.2 MeV) are in accordance with the experimental results as quoted in the particle data group (PDG 2016) [2]. The predicted masses of the S-wave charmonium states, 3^1S_0 (3990.8 MeV), 4^1S_0 (4262.1 MeV) and 5^1S_0 (4439.2 MeV), are in accordance with other model predictions [50,54,55]. The computed P-wave bottomonium states 2^3P_2 (10265.9 MeV), 2^3P_1 (10258.9 MeV) and 2^3P_0 (10234.7 MeV) are in good agreement with experimental [2] results of 10268.65 ± 0.22, 10255.46 ± 0.22 and 10232.50 ± 0.40 MeV, respectively. For charmonium, the predicted P-wave mass of 3921.2 MeV for the 2^3P_2 state is in very good agreement with the available experimental result of 3927.2 ± 2.6 MeV [2]. The masses of 3P, 4P and 1D to 4D states and their fine structure splitting for bottomonium and charmonium are in fairly good agreement with the available experimental results and other theoretical predictions. The predicted states such as $\chi_b(3P)$, $\chi_b(4P)$, $\Upsilon(3D)$, $\Upsilon(4D)$ and $\Upsilon(5D)$ of bottomonium and $\chi_c(2P)$ to $\chi_c(4P)$, 2D to 5D states of charmonium are not available experimentally.

In this paper, we have also examined the vector decay constant and leptonic decay widths for nS states of bottomonium and charmonium within the relativistic framework. The decay widths of $\Upsilon(nS) \to e^+e^-$ and $\psi(nS) \to e^+e^-$ are shown in Table 9. All the results for the vector decay constant and leptonic decay width are calculated without QCD corrections. The calculated leptonic decay widths for $\Upsilon(3S)$ and $\Upsilon(4S)$ are in good agreement with the available experimental data, but the calculated values for $\Upsilon(2S)$ are slightly higher than the experimental value. In the case of the $\psi(3S)$ state of charmonium, the vector decay constant and the leptonic decay width are slightly higher than the experimental result. Our results for $f_{J/\psi(1S)}$ and $f_{\psi(2S)}$ are in good agreement with the lattice QCD results of 399 ± 4 GeV and 143 ± 81 MeV, respectively [67]. It is observed that the leptonic decay widths decrease with radial excitations. From this we can conclude that the relativistic treatment is important for higher excited states.

To understand the structure of some of the newly found 'X Y Z' quarkonia-like—states with hidden charm and hidden bottom flavors, we consider here the possibilities for the mixing of $^3P_1$ and $^1P_1$ and of $^3S_1$ and $^3D_1$ iso-parity states. The calculated mixed states of $^3P_1$–$^1P_1$ and $^3S_1$–$^3D_1$ are listed in Tables 11 and 12 respectively. The corresponding leptonic decay widths of the 1^{--} admixture states are also listed in Table 11.

Now, we briefly summarize the structure of some of the newly found quarkonia-like states based on our results of the masses and the leptonic decay widths.

- The X(3940) has been observed in the $D^*\bar{D}$ channel with J^P value 1^+ but not in the $D\bar{D}$ decay mode [69]. Looking into its parity, the possible identification of this state

could be one of the charmonium-like states. However, the predicted 2P states are lower than this mass, while the 3P states are slightly higher than this mass. Based on our analysis of mixed states, we predict X(3940) as an 1^+ state with admixture of 2^3P_1 and 2^1P_1 charmonia.

- Similarly, we predict X(4020) as an admixture of 2^3P_1 and 3^1P_1 state with $J^P = 1^+$ having mass 4011.56 MeV.
- The Particle Data Group has renamed Y(4140) to X(4140) [2]. Many attempts are made to study this state. According to Ref. [70] this state might be a candidate of the tetra-quark state but because of the unknown value of J^P, its status is still not confirmed. According to our analysis it does not fit into the admixture of P-states. But it fits well with the pure charmonium 3^3P_0 state where one predicts its J^P value to be 0^+.
- The X(4350) state whose J^P value is not known experimentally is predicted as an admixture of 4^3P_1 and 3^1P_1 states having a mass of 4349.76 MeV or it might be a pure charmonium 4^1P_1 state with J^P value 1^+. Similarly, the X(10610) is also found to be an admixture of 4^3P_1 and 3^1P_1 states of bottomonium having a mass of 10595.63 MeV with J^P equal to 1^+.
- For the better identification of some of the 1^{--} states, we have considered both the predicted masses and their leptonic decay widths in accordance with our previous study [50] as the successive mass differences [(n−1)S − nS] as well as the leptonic decay widths of 1^{--} states of quarkonia, which have shown to follow a specific decreasing pattern, characteristic of the bound state.
- Accordingly, our predicted mass for the $\psi(3S)$ state as 4022.4 MeV and its leptonic decay width as 1.21 keV do not follow with the experimental mass of $\psi(3770)$ state and its experimental leptonic decay width of 0.262 ± 0.018 keV [2]. But according to our predicted mass of the 1^3D_1 state as 3745.3 MeV and its computed leptonic decay width of 0.27 keV, we have indications that $\psi(3770)$ is the right candidate for a pure charmonium 1^3D_1 state.
- In 2013, the Belle Collaboration updated the analysis of $e^+e^- \to J/\psi\pi^+\pi^-$ with a 967 fb^{-1} data sample and shows the invariant mass distribution of $J/\psi\pi^+\pi^-$, the distribution is fitted with two coherent resonances. The existence of Y(4008) state was further confirmed [71] consistent with Belle's previous results [26]. There are some theoretical approaches to understanding the structure of Y(4008) after Belle's confirmation [26]. Liu discussed some possibilities for the Y(4008), including both the (3S) charmonium states and the $D^*\bar{D}^*$ molecular state. For both possibilities, he found the branching ratio of $Y(4008) \to J/\psi\pi^0\pi^0$ is comparable with that of $Y(4008) \to J/\psi\pi^+\pi^-$ [72]. Li and Chao studied the higher charmonium states in the non-relativistic screened potential model, and they predicted the Y(4008) as the (3S) charmonium state [73]. Chen, Ye, and Zhang found that the Y(4008) is difficult to identify 3^3S_1 pure charmonium [74]. The Y(4008) was studied by Maiani, Piccinini, Polosa, and Riquer in their type-II diquark–antidiquark model, and interpreted it as a tetraquark state [75] and they have also assigned Y(4360) as the first radial excitations of Y(4008) tetraquark state. In [76], Zhou, Deng, and Ping also predicted the Y(4008) as a tetraquark state $cq\bar{c}\bar{q}$ with $J^{PC} = 1^{--}$ and $n^{2S+1}L_J = 1^1P_1$. They have used a color flux-tube model with a four-body confinement potential to interpret the status of Y(4008). According to Dian-Yong Chen, the Fano-like interference induces an extra broad structure in $Y(4008) \to \pi^+\pi^- J/\psi$ as a companion peak to Y(4260) and also it is explained why Y(4008), Y(4260) and Y(4360) are absent in the experimental data of the R value scan [77] and they have concluded that appearance of Y(4008) peak is due to the interference of $\psi(4160)/\psi(4415)$ with the continuum of $Y(4008) \to \pi^+\pi^- J/\psi$ [77]. However, very recently BESIII could not confirm the existence of Y(4008) [7]. In this context, Y(4008) is still a controversial state.

  In the present study, the predicted mass of Y(4008) is found to be close to 2^3D_1 charmonium state with just 8.6 % mixing with the 2^3S_1 charmonium state. However, the computed leptonic decay width of the admixture state (0.347 keV) is much lower than the experimentally reported value of 0.86 keV [72]. Thus by considering both the mass and the leptonic decay width together, it is difficult to confirm or understand the structure of Y(4008). We look forward to more refined experimental data for better understanding of this state.
- According to the present study, the state $\psi(4160)$ is found to be an admixture of 3^3D_1(60.8 %) and 3^3S_1 (39.2 %) states with its leptonic decay width as 0.534 keV, which is in accordance with the experimental result of 0.48 ± 0.22 keV [2].
- The state Y (4260) was observed by the BaBar Collaboration in the $J/\psi\pi^+\pi^-$ channel in the initial state radiation (ISR) process [28]. It was confirmed by CLEOc [30], Belle [26] and an additional analysis done by BaBar [78], with mass values varying in different analyses. The decay modes of the Y (4260) into J/ψ and other charmonium states indicate the presence of a $c\bar{c}$ content. From PDG [2], the masses of some radial excitations, $\psi(2S)$ and $\psi(1P)$ are well established, but the masses of $\psi(3S)$, $\psi(4S)$, $\psi(1P)$, $\psi(2P)$ and $\psi(1D)$ still need more experimental investigation. Some theoretical interpretations for the Y (4260) are hybrid mesons (mixing of $c\bar{c}$ and $c\bar{c}g$) [79–82], tetraquark state [83], hydrocharmonium [84–86], hadronic molecules of $\bar{D}D_1(2420) + c.c.$ [87], $\omega\chi_{c0}$ [88] etc. For the $\omega\chi_{c0}$ molecule, the predicted leptonic decay width is only about 23 eV [88]. By Llanes-

Estrad Y(4260) was proposed to be a conventional charmonium $\psi(4S)$ state and also estimated to have a leptonic decay width as 0.2–0.35 keV [89]. Wen Qin, Si-Run Xue and Qiang Zhao have predicted the upper limit of the Y (4260) leptonic decay width to be about 500 eV [90]. The LQCD also predicts the leptonic decay width as < 40 eV for a hybrid charmonium state [91].

According to new results from BESIII [7], Y(4260) is not a simple peak. This measurement of the $e^+e^- \to \pi^+\pi^- J/\psi$ cross section was done by using both a small number of high-statistical data points and a large number of low-statistics data points [7]. They found the resonance Y(4260) is described as a combination of two peaks Y(4220) and Y(4330) [7]. However, the structure and interpretations of Y(4220) and Y(4330) are not yet understood. Recently, Gao, Shen and Yuan have predicted that the value of the leptonic decay width for Y(4220) can be as large as 200 eV or even higher based on current information [92]. So the peaks observed by BESIII will provide more information as regards their structure. Thus the states Y(4260), Y(4220) and Y(4330) have opened up new challenges in the charm sector.

According to the latest PDG 2016 [2], the earlier state Y(4260) is now renamed as X(4260). We have analyzed the status of X(4260), Y(4220) and Y(4330) states.

According to the present study the Y(4220) state is not fit to be seen as a pure charmonium state but fit to be seen as an admixture of $(3^3D_1)(71.3\ \%)$ and $(3^3S_1)(28.7\ \%)$ states with its estimated leptonic decay width as 0.417 keV.

The second resonance reported by BES III, Y(4330) with mass 4326.8 ± 10 MeV, is close to our predicted 3^3D_1 state having a mass of 4300.6 MeV and a predicted leptonic decay width of 0.099 keV.

If we now consider X(4260) as a pure $\psi(4S)$ state with the predicted mass equal to 4266.4 MeV, then its leptonic decay width is predicted as 0.63 keV, which is higher than the upper limit of 0.500 keV [90]. And if we consider X(4260) as a mixed state of Y(4220) and Y(4330) with a mixing probability of 0.67 : 0.33, then its leptonic decay width has to be 0.258 keV. The recent experimental measurements of BESIII [93,94] suggests a comparatively very small leptonic decay width for X(4260) [88]. Thus, the X(4260) state can neither be identified as a pure state nor as a mixed state. The X(4260) state might be an exotic state or a hadronic molecular state. We require more experimental data for the confirmation of the X(4260) state.

- Another controversial state is Y(4360), having a J^P value 1^-, which has now been renamed as X(4360) [2]. This state may be a diquark–anti-diquark type tetraquark state or it may be a mixed S–D-wave charmonium state [95]. The present analysis suggests it to be a mixed 4^3S_1 and 4^3D_1 charmonium state with a leptonic decay width of 0.431 keV.
- X(4630) is compatible with our 1^{--} mixed charmonium state with an admixture of 5^3S_1 and5^3D_1 states having a mass of 4634 MeV and its predicted leptonic decay width as 0.117 keV.
- The structure of Y(4660) is also interesting because this state was neither observed in $e^+e^- \to \gamma_{ISR}p^+p^-J/\psi$ process, nor in the mass distributions of a $c\bar{c}$ in the final stage of e^-e^+ collision experiment [96]. Other theoretical approaches suggested it to be a molecular-like structure. According to latest PDG [2], Y(4660) has been renamed X(4660) and its $J^P = 1^-$ value suggests that it might be an admixture of 5^3S_1 and 5^3D_1 states, and we have predicted its leptonic decay width to be 0.110 keV. However, the status of these states is still a mystery and to resolve this we need more experimental results on their leptonic decay widths.
- The Particle Data Group has renamed $Y_b(10888)$ by $\Upsilon(10860)$ [2]. In our present study, by considering both its mass and leptonic decay width, we find it very difficult to assign it as the $b\bar{b}$, 5S state. Even if we consider it as an admixture of 5^3S_1 and 5^3D_1 states, its leptonic decay width is estimated to be equal to 0.096 keV, which is much lower than the experimentally reported value of 0.31 ± 0.07 keV [2]. So, the status of $Y_b(10888)$ or $\Upsilon(10860)$ as a conventional bottomonium state or an admixture of S–D states is doubted. More refined experimental observations of $\Upsilon(10860)$ can shed more light on the understanding of this state.

6 Summary

In the present paper we have proposed a quark model for hadrons. The approach is attractive due to its simplicity in applications to quarkonia and exotic hadrons. In our model for meson mass spectroscopy we have solved the Dirac equation to obtain the binding energy for individual quark/anti-quark. Further the mass of the bound state is computed by adding the binding energies of the quark and anti-quark with the addition of a center of mass correction.

In the last few years many states have been observed at B-factories (BaBar, Belle and CLEO), at proton–proton colliders (ATLAS, CMS, CDF, D0, LHCb), and at τ-charm facilities (CLEO-c, BES3) in the heavy quarkonium sector. These charmonium-like and bottomonium-like states have provided new challenges for theorists as well as for experimentalists because it reveals the inner mechanisms of hadrons. There is no confirmation regarding XYZ states as exotic states, molecular states and as regards a hybrid structure. We have predicted the status of a few unknown states as an admixture of two states having the same J^P values and predicted

their leptonic decay widths. The LHCb (CERN), BES-III (China), PANDA (FAIR, Germany; after 2018) and Belle (Japan) experiments are expected to pour more data in the quarkonium sector. With the help of advanced experimental facilities we hope to get valuable information related to the newly observed hadronic states. The theoretical predictions will be helpful for the experimental exploration of the hadronic states in the quarkonium sector.

Acknowledgements We acknowledge the financial support from DST-SERB, India (research project number: SERB/F/8749/2015-16).

Open Access This article is distributed under the terms of the Creative Commons Attribution 4.0 International License (http://creativecommons.org/licenses/by/4.0/), which permits unrestricted use, distribution, and reproduction in any medium, provided you give appropriate credit to the original author(s) and the source, provide a link to the Creative Commons license, and indicate if changes were made.
Funded by SCOAP[3].

References

1. N. Brambilla et al., Eur. Phys. J. C **71**, 1534 (2011)
2. C. Patrignani et al., Chin. Phys. C **40**, 100001 (2016)
3. Belle Collaboration, S.K. Choi, Phys. Rev. Lett. **91**, 262001 (2003)
4. L.I. Hai-BO, Pramana (Indian Academy of Sciences) **79**, 579 (2012)
5. C. Patrignani, T.K. Pedlar, J.L. Rosner, Annu. Rev. Nucl. Part. Sci. **63**, 21 (2013)
6. Z. Haddadi, for the BESIII Collaboration, J. Phys. Conf. Ser. **742**, 012013 (2016)
7. M. Ablikim et al., BESIII Collaboration, Phys Rev. Lett. **118**, 092001 (2017)
8. A. Adare et al., PHENIX Collaboration, Phys. Rev. C **84**, 054912 (2011). arXiv:1103.6269
9. C. Aidala, et al., PHENIX Collaboration, arXiv:1404.1873 (2014)
10. L. Adamczyk et al., STAR Collaboration, Phys. Rev. Lett. **111**, 052301 (2013). arXiv:1212.3304
11. L. Adamczyk et al., STAR Collaboration, Phys. Lett. B **735**, 127 (2014). arXiv:1312.3675
12. L. Adamczyk et al., STAR Collaboration, Phys. Lett. B **722**, 55 (2013). arXiv:1208.2736
13. B. Abelev et al., ALICE Collaboration, Phys. Rev. Lett. **109**, 072301 (2012). arXiv:1202.1383
14. S. Chatrchyan et al., CMS Collaboration, J. High Energy Phys. **1205**, 063 (2012). arXiv:1201.5069
15. S. Chatrchyan et al., CMS Collaboration, Phys. Rev. Lett. **109**, 222301 (2012). arXiv:1208.2826
16. S. Chatrchyan, et al., CMS Collaboration, Technical Report CMS-PAS-HIN-12-014. CERN, Geneva (2012)
17. S. Chatrchyan, et al., CMS Collaboration, Technical Report CMS-PAS-HIN-12-001. CERN, Geneva (2013)
18. E. Abbas et al., ALICE Collaboration, Phys. Rev. Lett. **111**, 162301 (2013). arXiv:1303.5880
19. B.B. Abelev et al., ALICE Collaboration, Phys. Lett. B **743**, 314 (2014). arXiv:1311.0214
20. A. Andronic, Nucl. Phys. A **931**, 135–144 (2014)
21. A. Rai, J.N. Pandya, P.C. Vinodkumar, J. Phys. G. Nucl. Part. Phys. **31**, 1453 (2005)
22. S. Patel, P.C. Vinodkumar, S. Bhatnagar, Chin. Phys. C **40**, 053102 (2016)
23. D. Ebert, R.N. Faustov, V.O. Galkin, Mod. Phys. Lett. A **18**, 601 (2003)
24. S. Eidelman (Budker Inst. and Novosi-Birsk State Univ.), B.K. Heltsley (Cornell Univ.), J.J. Hernandez-Rey (Univ. Valencia CSIC), S. Navas (Univ. Granada), C. Patrignani (Univ. Genova, INFN), Unpublished note, 18 Dec 2013 (2013)
25. S. Godfrey, S.L. Olsen, arXiv:0801.3867 [hep-ph]
26. C.Z. Yuan et al., Phys. Rev. Lett. **99**, 182004 (2007). arXiv:0707.2541 [hep-ex]
27. X.L. Wang et al., Belle Collaboration, Phys. Rev. D **87**, 051101(R) (2013)
28. B. Aubert et al., BABAR Collaboration, Phys. Rev. Lett. **95**, 142001 (2005). arXiv:hep-ex/0506081
29. B. Aubert et al., BABAR Collaboration, arXiv:0808.1543v2 [hep-ex]
30. Q. He et al., CLEO Collaboration, Phys. Rev. D **74**, 091104 (2006). arXiv:hep-ex/0611021
31. T.E. Coan et al., CLEO Collaboration, Phys. Rev. Lett. **96**, 162003 (2006). arXiv:hep-ex/0602034
32. B. Aubert et al., BABAR Collaboration, Phys. Rev. Lett. **98**, 212001 (2007). arXiv:hep-ex/0610057
33. X.L. Wang et al., Belle Collaboration, Phys. Rev. Lett. **99**, 142002 (2007). arXiv:0707.3699 [hep-ex]
34. G. Pakhlova et al., Belle Collaboration, Phys. Rev. Lett. **101**, 172001 (2008). arXiv:0807.4458 [hep-ex]
35. K.-F. Chen et al., Belle Collaboration, Phys. Rev. D **82**, 091106 (2010). arXiv:0808.2445 [hep-ex]
36. K.F. Chen et al., Belle Collaboration, Phys. Rev. Lett. **100**, 112001 (2008). arXiv:0710.2577 [hep-ex]
37. B. Aubert et al., Phys. Rev. D **71**, 071103 (2005)
38. LHCb Collaboration, R. Aaij et al., Phys. Rev. Lett. **110**, 222001 (2013)
39. T. Barnes, F.E. Close, E.S. Swanson, Phys. Rev. D **91**, 014004 (2015)
40. J.L. Rosner et al., CLEO Collaboration, Phys. Rev. Lett. **95**, 102003 (2005). arXiv:hep-ex/0505073
41. S. Dobbs et al., CLEO Collaboration, Phys. Rev. Lett. **101**, 182003 (2008). arXiv:0805.4599 [hep-ex]
42. I. Adachi et al., Belle Collaboration, Phys. Rev. Lett. **108**, 032001 (2012). arXiv:1103.3419 [hep-ex]
43. P.C. vinodkumar, K.B. Vijayakumar, S.B. Khadkikar, Pramana J. Phys. **39**, 47 (1992)
44. M. Shah, B. Patel, Eur. Phys. J. C **76**, 36 (2016)
45. M. Shah, B. Patel, P.C. Vinodkumar, Phys. Rev. D **90**, 014009 (2014)
46. M. Shah, B. Patel, P.C. Vinodkumar, Phys. Rev. D **93**, 094028 (2016)
47. G. Aruldhas, Quantum Mechanics. in *PHI Learning Private Limited* (New Delhi, India, 2012), pp. 396–403
48. W. Greiner, in *Relativistic Quantum Mechanics-Wave Equations* (Springer-Verlag, Berlin, 1990), pp. 169–172
49. A.P. Monteiro, K.B. Vijaya Kumar, Nat. Sci. **2**, 1292 (2010)
50. M. Shah, A. Parmar, P.C. Vinodkumar, Phys. Rev. D **86**, 034015 (2012)
51. S.F. Radford, W.W. Repko, Nucl. Phys. A **865**, 69 (2011)
52. W.-J. Deng, H. Liu, L.-C. Gui ,X.-H. Zhong, arXiv:1607.04696v2 [hep-ph]
53. A.E. Bernardini, C. Dobrigkeit, J. Phys. G. Nucl. Part. Phys. **29**, 1439–1449 (2003)
54. B.-Q. Li, K.-T. Chao, Phys. Rev. D **79**, 094004 (2009)
55. T. Barnes, S. Godfrey, E.S. Swanson, Phys. Rev. D **72**, 054026 (2005)
56. T. Kawanai, S. Sasaki, arXiv:1503.05752
57. K. Bhaghyesh, B. Vijaya Kumar, A.P. Monteiro, Phys. G. Nucl. Part. Phys. **38**, 085001 (2011)
58. O. Lakhina, E.S. Swanson, Phys. Rev. D **74**, 014012 (2006)

59. B. Patel, Ph.D Thesis (2009)
60. A.K. Rai, J. Phys. Conf. Ser. **374**, 012017 (2012)
61. S.F. Radford, W.W. Repko, Phys. Rev. D **75**, 074031 (2007)
62. P.C. Vinodkumar, J.N. Pandya, V.M. Bannur, S.B. Khadkikar, Eur. Phys. J. A **4**, 83 (1999)
63. S. Louise, J.-J. Dugne, J.-F. Mathiot, Phys. Rev. Lett. B **472**, 357 (2000)
64. K.-T. Chao, H.-W. Huang, Y.-Q. Liu, arXiv:hep-ph/9503201v1
65. P.C. Vinodkumar, Eur. Phys. J. C **76**, 356 (2016)
66. B.H. Yazarloo, H. Mehraban, EPL **115**, 21002 (2016)
67. J.J. Dudek, R.G. Edwards, D.G. Richards, JLab Lattice group, Phys. Rev. D **73**, 074507 (2006). arXiv:hep-ph/0601137
68. F. Hui-feng, X. Chen, G.-L. Wang, Phys. Lett. B **692**, 312 (2010)
69. W. Sreethawong, K. Xu, Y. Yan, arXiv:1306.2780v4 [hep-ph]
70. Z.-G. Wang, Y.-F. Tian, arXiv:1502.04619v1 [hep-ph]
71. Z.Q. Liu et al., Phys. Rev. Lett. **110**, 252002 (2013)
72. X. Liu, Eur. Phys. J. C **54**, 471–474 (2008)
73. B.-Q. Li, K.-T. Chao, Phys. Rev. D **79**, 094004 (2009)
74. D.-Y. Chen, J. He, X. Liu, Phys. Rev. D **83**, 054021 (2011)
75. L. Maiani, F. Piccinini, A.D. Polosa, V. Riquer, Phys. Rev. D **89**, 114010 (2014)
76. P. Zhou, C.-R. Deng, J.-L. Ping, Chin. Phys. Lett. **32**(10), 101201 (2015)
77. D.-Y. Chen, X. Liu, X.-Q. Li, H.-W. Ke, Phys. Rev. D **93**, 014011 (2016)
78. J.P. Lees, BaBar, Phys Rev. D **86**, 051102 (2012). arXiv:1204.2158 [hep-ex]
79. F. Iddir, L. Semlala, arXiv:hep-ph/0611183
80. S.L. Zhu, Phys. Lett. B **625**, 212 (2005)
81. F.E. Close, R.P. Page, Phys. Lett. B **628**, 215 (2005)
82. E. Kou, O. Pene, Phys. Lett. B **631**, 164 (2005)
83. L. Maiani, V. Riquer, F. Piccinini, A.D. Polosa, Phys. Rev. D **72**, 031502 (2005)
84. M.B. Voloshin, Prog. Part. Nucl. Phys. **61**, 455 (2008)
85. S. Dubynskiy, M.B. Voloshin, Phys. Lett. B **666**, 344 (2008)
86. S. Dubynskiy, A. Gorsky, M.B. Voloshin, Phys. Lett. B **671**, 82 (2009)
87. G.-J. Ding, Phys. Rev. D **79**, 014001 (2009)
88. L.Y. Dai, M. Shi, G.Y. Tang, H.Q. Zheng, Phys. Rev. D **92**, 014020 (2015)
89. F.J. Llanes-Estrada, Phys. Rev. D **72**, 031503 (2005)
90. W. Qin, S.-R. Xue, Q. Zhao, Phys. Rev. D **94**, 054035 (2016)
91. Y. Chen, W.F. Chiu, M. Gong, L.C. Gui, Z. Liu, Chin. Phys. C **40**, 081002 (2016)
92. X.Y. Gao, C.P. Shen, C.Z. Yuan, Phys. Rev. D **95**, 092007 (2017)
93. M. Ablikim et al., [BESIII Collaboration], Phys. Rev. Lett. **114**(9), 092003 (2015)
94. M. Ablikim et al., [BESIII Collaboration], Phys. Rev. D **93**(1), 011102 (2016)
95. Z.-G. Wang, arXiv:1601.05541v3 [hep-ph]
96. F.-K. Guo, J. Haidenbauer, C. Hanhart, U.-G. Meiner, arXiv:1005.2055v1 [hep-ph]